Deadbeat State Space Control of Spinning Satellite[#]

Ezzeddin M. Elarbi[1] and Saad M. Issa*[2]

Abstract: The colony of a celestial universe has become foremost task for many countries in the late decades. The spinning attitude control for economical satellite operation is widely used. This paper shows a successful implementation of state space technique to inherently unstable satellite spun around longitudinal axis. Full-state feedback and reference input with full-state feedback are compared for deadbeat response. The state space control gains are tuned to satisfy controllability conditions. Observability conditions are checked for better tracking of attitude spinning angle to step input with the aim to achieve a robust spin stabilization of the satellite manoeuvre. Satisfactory deadbeat specifications are obtained based on reference input with full-state feedback. However, full-state feedback implements reasonable design gains and it appears to be slower in judgment with reference input with full-state feedback gains. The simulation and analytical results are well agreed based on dominant second-order poles.

Keywords: Spinning Satellite Stabilization, Deadbeat Control, State Space, Pole Placement Method, FSF and RIFSF controllers.

Nomenclatures

T_x, T_y, T_z	Torques around x, y and z axes [N m].
I_x, I_y, I_z	Mass moment of intertie around x, y and z axes [Kg m²].
$K = \begin{bmatrix} K_1 & K_2 \end{bmatrix}$	Full state feedback vector
$\alpha_x, \alpha_y, \alpha_z$	Angular accelerations Around x, y and z axes [rad/sec²].
$\overline{N}$	Overall reference input gain
ω_n	Undamped frequency [rad/sec].
N_u	Explicit reference input gain
$\omega_x, \omega_y, \omega_z$	Angular velocities around x, y and z axes [rad/sec].
$N_x = \begin{bmatrix} N_{x1} & N_{x2} \end{bmatrix}$	Reference input gains corresponds with full state feedback vector

1. Introduction

The adventure into space is usually undertaken for scientific missions, communications, surveillances and reconnaissance. The pioneering space explorations are made by the soviet union and united states at the late of 1950s [1]. By the end of past century it has seen partnerships many countries such as Japan and Europe to invade the space. Lastly, Chine and India ride the race into space due to the availability of various resources. Spinning attitude control is one of strategies for long life mission for more than 40 years. Propulsion system thrusters are fired only occasionally to make desired changes in the spin-stabilized attitude. At the present time, most of the satellite attitude controls in practical world are based on a proportional-integral-derivative (*Pid*) controller algorithm [2]. The state space (*SS*) method is a simple technique to describe satellite

spun around longitudinal axis. The SS method has been in a use for over 100 years and is introduced to control designs in the ate 1950s by R. E. Kalman [3].

Beginning in the late 1950s and early 1960s Kalman introduced the ideas of state-variables, controllability and observability. Zadeh and Desoer had a significant impact in promoting the state-space method. During the 1980s reliable numerical methods were developed for dealing with state-variable designs and computer-aided software for control design [4]. Since the invention of Matlab by Cleve Miler huge applications for control design were made. The state-variable methods were gaining momentum particularly in the US. Research groups in England led by Rosenbrock, MacFarlane, and Munro extended to multi-input multi-output systems. In the end of the 1980s the frequency domain method is used in connection with state-variable method as powerful approach [5]. The state-variable methods were found more computationally advantageous than the frequency domain method [6].

This paper is devoted to implement *SS* controller algorithms to unstable spinning satellite. The performance of Reference Input with Full State Feedback (*RIFSF*) and Full State Feedback (*FSF*) controller are examined for deadbeat specifications. A Matlab framework of M-file batch and Simulink is used to model, simulate and control spinning satellite.

2. Mathematical model

The brief demonstrations of satellite problem descriptions, control algorithms and implementations will be described below. Figure.1 illustrates the diagram of a spinning satellite with SS controller implementation. The operator is just Matlab-M-file script used to command Matlab-Simulink to perform the simulation tasks and return back the results for post processing. The SS controller block is used to implement one time *RIFSF* and another time *FSF* controller.

_____

[1,2] *Faculty of Engineering, University of Tripoli, Libya*
* Corresponding Author: Email: sissa@aerodept.edu.ly
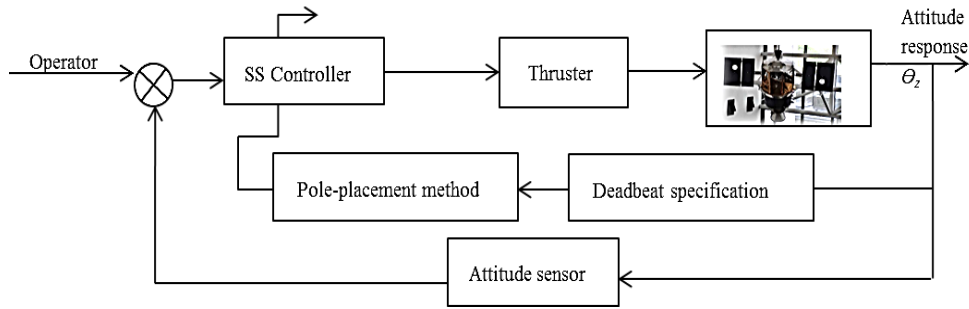
Figure 1. A schematic of spinning satellite control based on SS algorithm

A. Satellite Dynamic Model:

The satellite under consideration is an axis-symmetric rigid satellite of evenly distributed masses and space disturbance free. Of particular intention, the satellite is considered inherently unstable due to two poles at the origin. The satellite moment of inertia matrix is given by [7].

$$\begin{bmatrix} I_x & I_{xy} & I_{xz} \\ I_{xy} & I_y & I_{yz} \\ I_{xz} & I_{yz} & I_z \end{bmatrix} = \begin{bmatrix} 1000 & 0 & 0 \\ 0 & 1000 & 0 \\ 0 & 0 & 1000 \end{bmatrix} kgm^2$$

The satellite cannot keep its balance status and it could not come back to its initial orientation until controller is implemented. The non-linear equations of satellite motion can be shown as [8].

$$T_x = I_x \alpha_x - \left(I_y - I_z\right)\omega_y \omega_z$$
$$T_y = I_y \alpha_y - \left(I_z - I_x\right)\omega_z \omega_x \qquad (1)$$
$$T_z = I_z \alpha_z - \left(I_x - I_y\right)\omega_x \omega_y$$

Highly nonlinear characteristics of satellite dynamic system are linearized in a form of double-integral plant. There exists a linearized set of equation of motion, the coupling terms of angular velocities may be neglected for a small roll, pitch and yaw attitudes [9].

$$T_x = I_x \alpha_x$$
$$T_y = I_y \alpha_y \qquad (2)$$
$$T_z = I_z \alpha_z$$

To model the satellite spinning around the longitude axis where the moment of inertia is the largest, equation (2) will be modelled as

$$T_z = I_z \alpha_z = I_z \dot{\omega}_z = I_z \ddot{\theta}_z \qquad (3)$$

Because the system is linear, the step response can be derived for any input amplitude. The state-variable method is used to describe the satellite dynamics. A set of first-order differential equations in the vector-valued state of the system is composed below

$$x_1 = \theta_z$$
$$\dot{x}_1 = x_2 = \dot{\theta}_z = \omega_z \qquad (4)$$
$$\dot{x}_2 = \ddot{\theta}_z = \alpha_z = \frac{T_z}{I_z} + M_d$$

Where x_1 and x_2 are state variables, and θ_z is the spinning angular displacement around z axis.
The SS form can be given by

$$\left.\begin{array}{c} \dot{x} = Ax + Bu \\ \theta_z = Cx + Du \end{array}\right\} \qquad (5)$$

Where u is control effort and A is system matrix, B is input matrix, C is output matrix and D is direct transmission matrix, which are:

$$A = \begin{bmatrix} 0 & 1 \\ 0 & 0 \end{bmatrix}, B = \begin{bmatrix} 0 & \dfrac{1}{I_{zz}} \end{bmatrix}^T, C = \begin{bmatrix} 1 & 0 \end{bmatrix} \ and \ D = \begin{bmatrix} 0 \end{bmatrix}$$

In this study external disturbance (M_d) represented the solar pressure is not considered.

B. Control Law Algorithms:

Two concepts of control design working in connection with SS method are tested. *FSF* and *RIFSF* are applied and compared to assign a set of pole locations for the closed-loop system that is satisfactory dynamic transient response.

1) FSF:

$$u = -Kx = -\begin{bmatrix} K_1 & K_2 & \dots & K_n \end{bmatrix} \begin{bmatrix} x_1 \\ x_2 \\ \vdots \\ x_n \end{bmatrix} \qquad (6)$$

The transfer function of spinning satellite implementing FSF controller can be expressed as

$$\frac{x_1}{r} = \frac{\theta_z}{r} \frac{1}{I_z s^2 + K_2 s + K_1} \qquad (7)$$

Obviously, *FSF* implementation has two poles which are directly influenced by the satellite design, i.e., the moment of inertia and control gains.

2) RIFSF:

For zero steady state error to step input, introducing the reference input into the system results in changing the control law as follows

$$u = -Kx + \overline{N}r = -\begin{bmatrix} K_1 & K_2 & \dots & K_n \end{bmatrix} \begin{bmatrix} x_1 \\ x_2 \\ \vdots \\ x_n \end{bmatrix} + \overline{N}r \qquad (8)$$

$$\overline{N} = N_u + K N_x \qquad (9)$$

$$\begin{bmatrix} N_x \\ N_u \end{bmatrix} = \begin{bmatrix} A & B \\ C & D \end{bmatrix}^{-1} \begin{bmatrix} 0 \\ 1 \end{bmatrix} \qquad (10)$$

The transfer function of spinning satellite implementing RIFSF controller can be expressed as

$$\frac{x_2}{r} = \frac{\theta_z}{r} \frac{N_{x1}K_1 + N_{x2}K_2}{I_z s^2 + K_2 s + K_1} \qquad (11)$$

Again, *RIFSF* implementation has two poles which are directly influenced by the satellite design, i.e., the moment of inertia and control gains. However, the reference input constants have an implicit effect on the system performance as they appear as gain in the numerator.

C. Pole Placement Method

Using Eq.(6) the Eq.(5) becomes

$$\dot{x} = Ax - BKx \qquad (12)$$

The characteristic equation of the closed-loop system is

$$\det[sI - (A - BK)] \qquad (13)$$

An nth order polynomial in s containing the gains K1,…, Kn . Assuming the desired pole roots locations are

$$s = s_1, s_2, \ldots, s_n \qquad (14)$$

The corresponding control characteristic equation is

$$(S - S_1)(S - S_2).(S - S_n) = 0 \qquad (15)$$

The *K* vector is obtained by matching coefficients of Eq.(15) with the characteristic equations of Eqs.(7) and (11).
The dominant second order poles approach is considered here due to feasibility when higher order characteristic equations. In this method the poles are selected to satisfy the two conditions of controllability and observability.
The controllability matrix ς is computed as

$$\varsigma = \begin{bmatrix} B & AB & \ldots & BA^{n-1} \end{bmatrix}^T \qquad (16)$$

The system is said to be controllable for controllability matrix ς is non-singular.
The observability matrix O is calculated by

$$O = \begin{bmatrix} C & CA & \ldots & CA^{n-1} \end{bmatrix}^T \qquad (17)$$

The system is said to be observable for the observability matrix *O* is non-singular.

D. Model and Simulation

The implementations of *FSF* and *RIFSF* controller into spinning satellite dynamic model are schematically shown in (Figures. 2 & 3). A Matlab M-file script was used to provide workability to simulation model. The results obtained from the simulations are returned back to the script to post process them. The uncontrolled satellite has transfer function

$$Uncontrolled \ satellite : \frac{x_1}{r} = \frac{\theta_z}{r} = \frac{1}{5000s^2}$$

Where r is reference input command and the overall transfer functions of FSF and RIFSF controllers for a spinning satellite is given respectively.

$$FSF \ comtroller : \frac{x_1}{r} = \frac{\theta_z}{r} = \frac{1}{5000s^2 + 125s + 1}$$

and

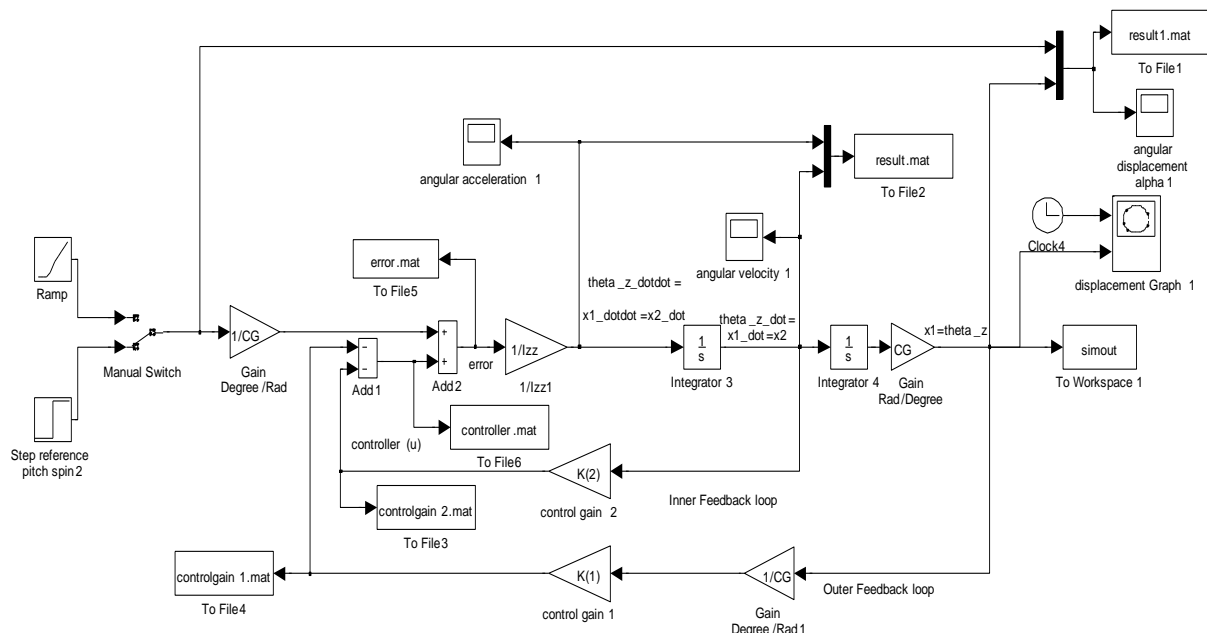$$RIFSF \ comtroller : \frac{x_1}{r} = \frac{\theta_z}{r} = \frac{80000}{5000s^2 + 36000s + 80000}$$

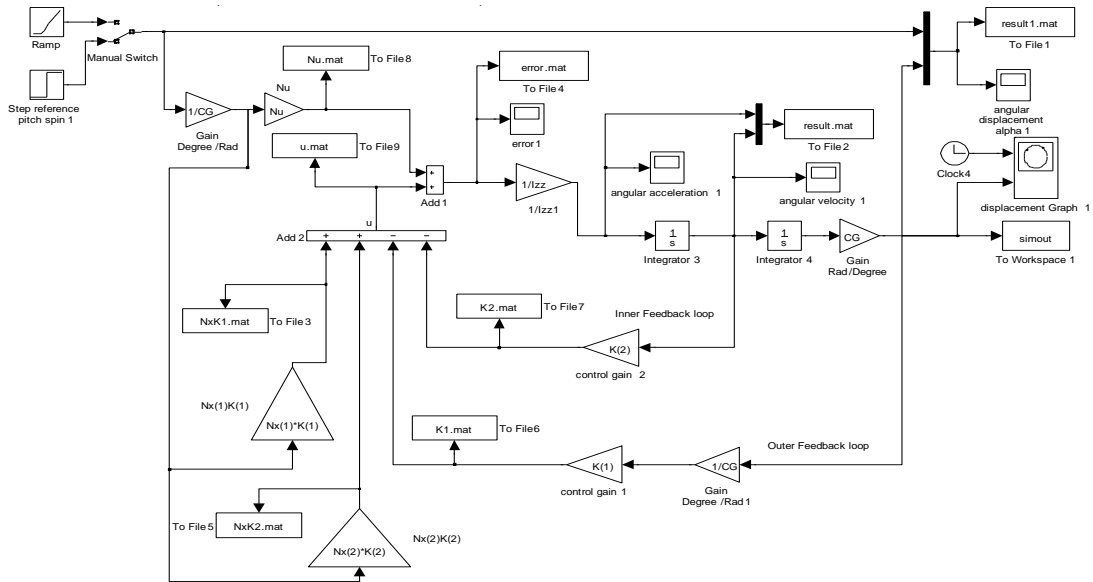**Figure 2**. A simulation diagram of *FSF* controller of spinning satellite

Figure 3. A simulation diagram of *RIFSF* controller of spinning satellite

3. Results and Discussions

The main results obtained in this study, are shown and a brief discussions are outline to elucidate the implication of the results.

E. System Eigenvalues

Figure.4 shows the root locus comparisons before implementing control algorithms with *FSF* and *RIFSF* controllers. Two poles at the origin of uncontrolled satellite make the spinning unstable. Stable eigenvalues of -3.6000 ± 1.7436i and -0.0125 ± 0.0066i are produced by *RIFSF* and *FSF* controllers respectively. For compact root locus comparisons with uncontrolled satellite and *FSF* controller, *RIFSF* gains are

normalised by 100. Cleary, just the real part of eigenvalues of *RIFSF* controller is normalised by 100 but the imaginary part is normalised by about 4.5. The locations of eigenvalues of uncontrolled satellite are moved by *RIFSF* and *FSF* controllers to the left hand side of s-plane but they are not too far from the original locations based on *FSF* controller. Evidently, *RIFSF* controller has more stable roots than *FSF* controller since the eigenvalues are far away in the left hand side of s-plane. Figure.5 shows a close up of root locus of uncontrolled satellite and *FSF* controllers. Although the real part of *FSF* eigenvalues are too close to the poles of uncontrolled satellite the imaginary part of *FSF* eigenvalues produces damped oscillation to unstable response of spinning satellite.
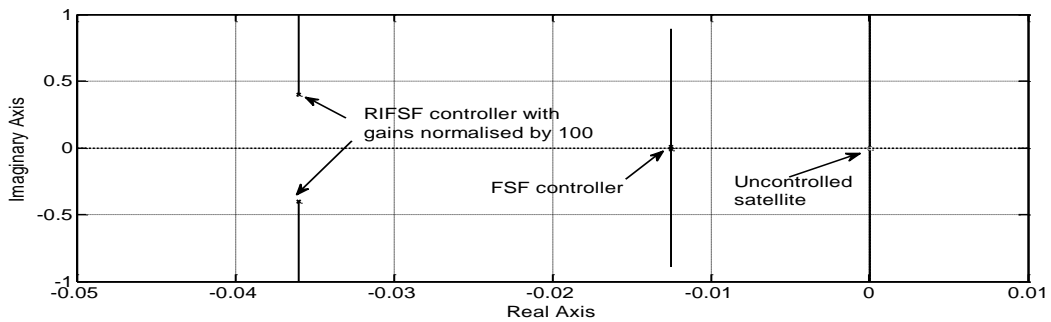

Figure 4. Root locus of uncontrolled satellite with *RIFSF* and *FSF* controllers
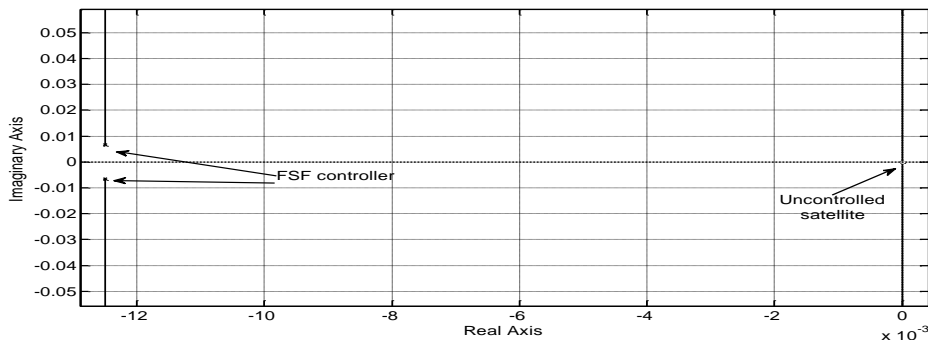

Figure 5. A close up view of root locus of uncontrolled satellite and *FSF* controller

F. Controller Gain Contribution

The contributions of each part of controller effort u ($N_{x1}K_1$, $N_{x2}K_2$, N_u, $K_1\theta_z$ and $K_2\dot{\theta}_z$) is investigated based on both *RIFSF* and *FSF* control implementations to uncontrolled spinning satellite. Figure.6 shows the contributions of *FSF* controller gains whereas (Figure.7) displays the contributions of *RIFSF* controller gains. The convergence of *FSF* control effort u occurs too late at about 400 sec, shown by starred line. The contribution of $K_2\dot{\theta}_z$ part (diamond line) has the averaged value of 0.0175 which is eliminated by -0.0175 produced with

$K_1\theta_z$ part (squared line). On the contrary, a fast convergence is obtained from *RIFSF* control effort u at an early time. Clearly, a fluctuating convergence around zero is seen by a starred line in (Figure.8) and the most contribution to u comes from $K_2\dot{\theta}_z$ part (diamond line). However, the contributions of N_u (triangular mark) and $N_{x2}K_2$ (plus mark) are considerably small. Nevertheless, the quite large contribution of $N_{x1}K_1$ (circled line) is cancelled with $K_1\theta_z$ part (squared line).
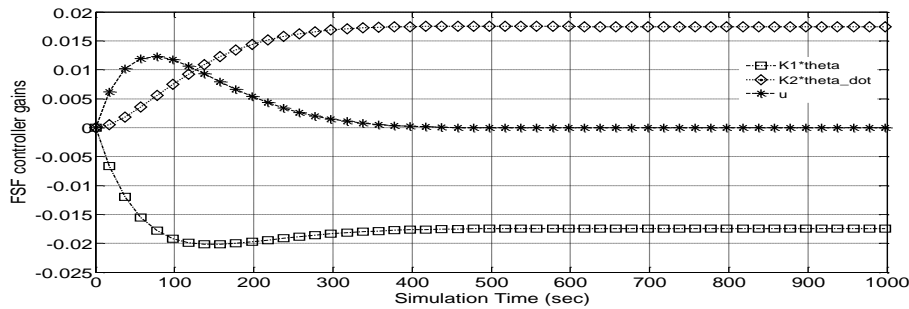
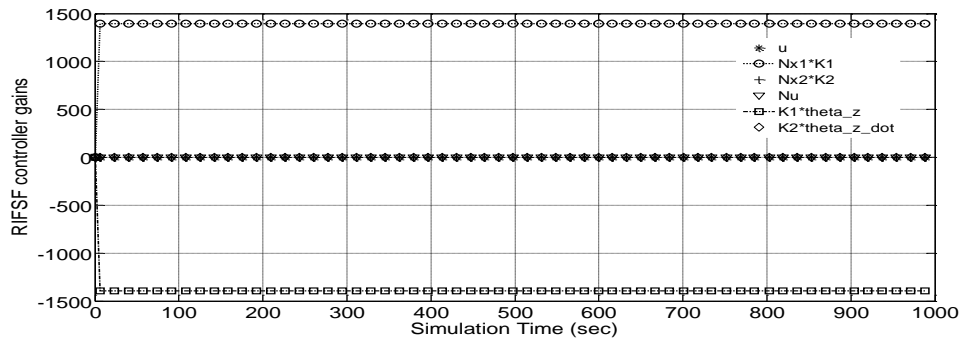Fig. 6 The contributions of *FSF* controller gains

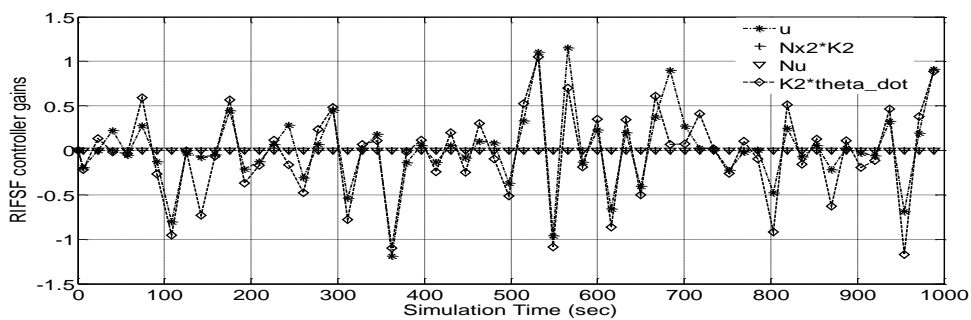**Figure 7.** The contributions of RIFSF controller gains

Figure 8. A close up view of the contributions of *RIFSF* controller gains

G. Deadbeat Response

A comparison of the performance of *FSF* and *RIFSF* controllers for a spinning satellite is shown in (Figure.9). Clearly, *RIFSF* performs well to meet the deadbeat specifications. Although *RIFSF* controller adequately tracks unity step input command it implements expansive impractical gains. However, *FSF* controller is not too bad for practical implementations since it deploys reasonable gains. A close up view of the response obtained by *RIFSF* and *FSF* controllers during the simulation time between 0-450 sec is shown in (Figure.10). Obviously, *FSF* is slower than *RIFSF* in terms of rise and settling times. Figure. 11 shows a comparison of

steady state convergence between *FSF* and *RIFSF* controllers. Apparently, *RIFSF* controller promptly shows steady state behaviour in a comparison with *FSF* controller which converges at approximately 800 sec. An average of zero steady state error is approximately produced by *RIFSF* controller in contrast to *FSF* controller which produces about 0.4% steady state error. The smooth convergence which is seen from *FSF* controller implementation refers to the contribution seen by the control effort u shown in (Figure.8). However, the fluctuating convergence based on *RIFSF* controller implementation (Figure. 11) is due to that was produced by the control effort u as seen in (Figure. 8).

The simulation and analytical results are agreed well based on dominant second-order poles. As early shown, *RIFSF* and *FSF* have dominate poles at -3.6000 ± 1.7436i and -0.0125 ± 0.0066i respectively. Standard performance measures are usually defined in terms of the step response. The swiftness of response is measured by the peak time T_p and rise time T_r. However, the track to desired response is examined by the settling time T_s and the percent overshoot $P.O$. The peak time TP is calculated by

$$T_p = \frac{\pi}{\omega_n \sqrt{1-\zeta^2}} \quad (18)$$

The liner approximation of analytical expression of rise time Tr can be found by

$$T_r = \frac{2.16\zeta + 0.6}{\omega_n} \quad (19)$$

The settling time TS for which the response remains within 2% of the final values is given by

$$T_s = \frac{4}{\zeta\omega_n} \quad (20)$$

The present overshoot is found by

$$P.O. = 100e^{-\zeta\pi/\sqrt{1-\zeta^2}} \quad (21)$$

Table (1) shows a comparison between the simulation results obtained from *RIFSF* controller for spinning stabilisation satellite and analytical calculations based on Eqs. (18-21). Table (2) shows a comparison between the simulation results obtained from FSF controller for spinning stabilisation satellite and analytical calculations based on Eqs. (18-21). *FSF* controller has the damping ratio ζ of 0.885 and the undamped frequency ω_n of 0.014 rad/sec versus 0.9 and 4 rad/sec associated with *RIFSF* controller. Those dynamic parameters are found based on the conditions of controllability C and observability O matrices not being singular, i.e. Eqs. (16-17).
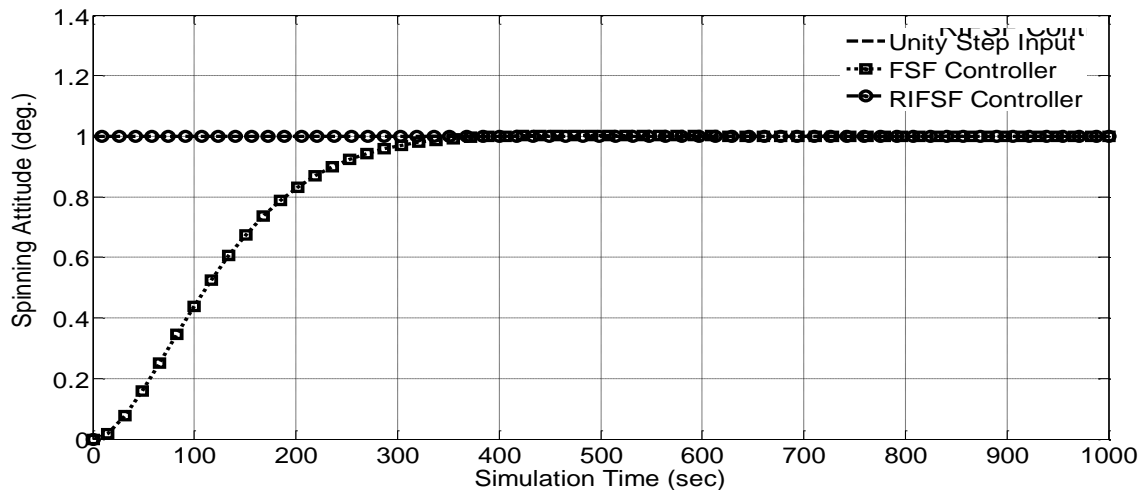
Table 1. A performance comparison of RIFSF controller and analytical calculations

Category	$T_p (sec)$	$T_r (sec)$	$T_s (sec)$	$P.O.$ %
RIFSF controller	1.7206	0.7754	1.1023	0.285
Analytical calculation	1.8018	0.6360	1.1111	0.255

Overall, a reasonable agreement is found between the simulation results and analytical calculations. The discrepancy between *RIFSF* controller and analytical calculation in T_r shown in Table (1) may refer to the liner approximation of analytical expression Eq. (19), particularly for $\zeta > 0.77$ [6]. *RIFSF* controller produces so swifter and more accurate response than *FSF* controller for spinning stabilisation satellite. A satisfactory deadbeat response is seen from *RIFSF* controller in terms of overshoot and steady state error. As may be noticed, the settling time is smaller than the peak time for *RIFSF* controller due to the deadbeat specifications met.

Table 2. A performance comparison of FSF controller and analytical calculations

Category	$T_p (sec)$	$T_r (sec)$	$T_s (sec)$	$P.O.$ %
FSF controller	477.60	174.10	319.60	0.285
Analytical calculation	477.20	177.62	319.65	0.255

Figure 9. Deadbeat response of angular displacement attitude to unit step input command
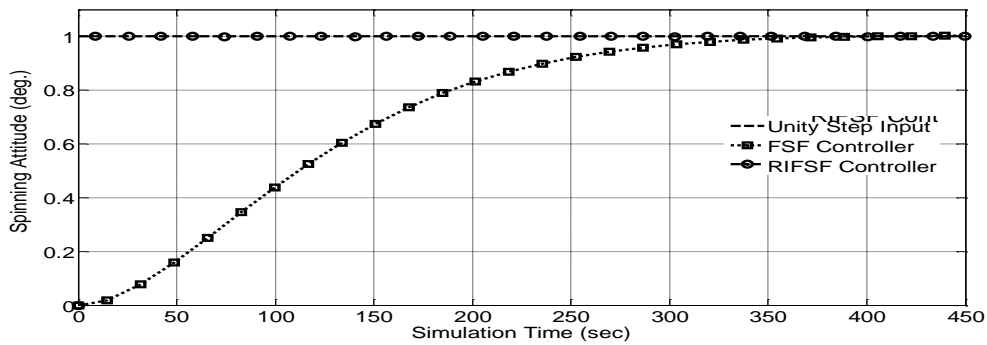
Figure 10. Zooming in view of angular displacement attitude response.
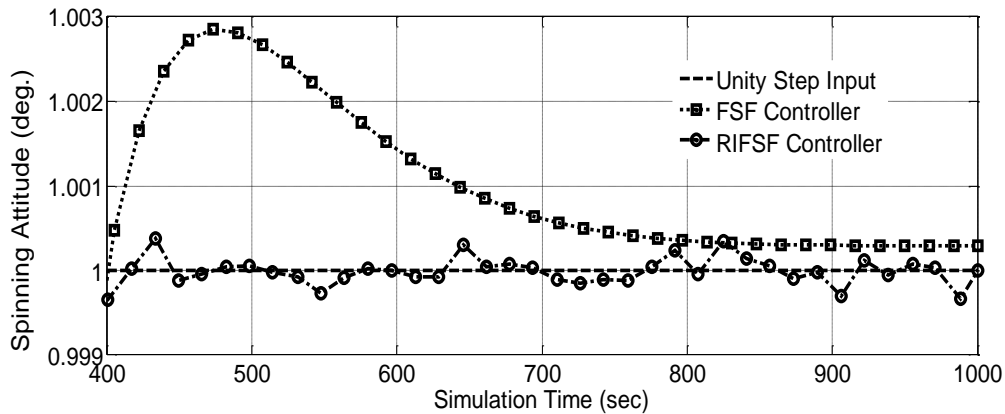

Figure 11. *FSF* vs *RIFSF* for a steady state convergence

4. Conclusions

This paper has been devoted to model and control spinning satellite. The satellite is intentionally chosen in an unstable mode. The aim has been to achieve a robust spin stabilization of the satellite manoeuvre. A successful implementation of two categories of *SS* control algorithms is achieved for a satisfactory performance of spinning satellite. *FSF* controller is compared with *RIFSF* arrangement for deadbeat response to step input command. To obtain feasible values of angular velocity, ramp angular displacement command is used to excite the spinning system of a satellite. For the validation of the simulation model, the most significant results obtained from the simulation are compared with analytical results based on dominant second-order poles of 0.9-damping ratio.

Satisfactory agreements are found in terms of overshoot, rise time, settling time and steady state response. Although *RIFSF* meets reasonable deadbeat specifications; overshoot of 0.2%, rise time of 0.65 sec, settling time of 1.2 sec and zero steady state error, it uses impracticable large gains in comparison with FSF which shows a humble deadbeat tracking in terms of a slow response. Thus *RIFSF* is expansive, too accurate but reliable and fast whereas FSF is slow but cheap. However, those controller gains are not unique and they depend on the optimization relaxations. The system has very good performance and come back to its initial orientation quickly when the disturbances are zero.

Future study may be formulated to use reduced-order estimator method to confirm the selected root locations. In case of space disturbance is not excluded as they appear in a real world *SS* control algorithms may not be robust enough to eliminate such external disturbance effects. Therefore, *SS* controller may not be used in practical world. H_∞ robust attitude controller may be designed to compensate such problem.

References

[1] Gene F. Frankin, J. David Powell, and Abbas Emami-Naeini (2010). Feedback Control of Dynamic Systems. 6th ed. Pearson Prentice HallTM.

[2] Buckley, G.J. (1990). Modern Control Started with Ziegler-Nichols Tuning. Control Engineering, 2nd Edition, Vol. 37, No. 12, pp. 11-17.

[3] Wittenmark, B. (1979). Self -tuning PID Controllers Based on Pole Placement. Lund Inst. of Technology. Report No. TFRT-7179.

[4] Kuo, Benjamin C (1994). 1930- MATLAB tools for control system analysis and design. Englewood Cliffs, NJ. Prentice Hall, 0130346462

[5] Tsiotras, P. 1996). Stabilisation and Optimality Results for the Attitude Control Problem. Journal of Guidance, Control, and Dynamics, Vol. 19, No. 4.

[6] Dorf, C.R. (1989). Modern Control Systems. 5th edition Reading, Ma. Addison- Wesley

[7] E. Finlay-Freundlich (1958). Celestial Mechanics. Pergamon press.

[8] Fortescue, M. (1996). Spacecraft Systems Engineering. McGraw Hill.

[9] Peter Fortescue. (1994). Spacecraft Systems Engineering. Wiley Publishers.